Supporting Information

Mythreye and Blobe 10.1073/pnas.0812879106

SI Methods

Cell Culture, Transfection, Adenoviral Infection and Reagents. Phosphorylated Smad2 (pSmad2), Smad2, Cdc42, and Rac1 antibodies were from Cell Signaling Technology (Catalog Nos. 3101, 3103, 2462, 2465) and pan-neutralizing-TGF-β antibody was obtained from R&D Systems. GST-PAK-CRIB-fusion protein was purified as previously described (1). GFP-tagged N17Cdc42 and N17Rac1 recombinant adenoviruses were obtained from George E. Davis (University of Missouri-Columbia, Columbia, MO) and prepared as described (2). Titers of virus ranged between 10^9 to 10^{14} infectious units per mL. All adenoviral infections were done at a multiplicity of infection of 50 for all constructs. β-arrestin2-knockdown experiments were conducted using the siRNA sequence targeting human β-arrestin2 (3).

siRNA to Smad2 was performed using the ON-TARGET plus siRNA target sequence GAAUUGAGCCACAGAGUAA to human Smad2 from Dharmacon. Cells were transfected for 48 h with either siRNA to Smad2 or control before harvesting for Western analyses and migration assays as described in *Materials and Methods*.

Immunoflourescence. The cells were fixed in 4% paraformaldehyde and permeabilized with 0.1% Triton X for 5 min. Blocking was performed with 1% BSA, and cells were then incubated with a 1:50 dilution of phalloidin conjugated to either Texas Red (Molecular Probes) or Alexa 488 for 20 min. Immunofluorescence images were obtained using a Nikon inverted microscope.

Transwell Migration Assays. The pharmacological reagents, including 1 μm of cytochalasin D, 100 μm of blebbistatin, 10 μg/mL of pan-neutralizing-TGF-β antibody, 40–60 ng of soluble form of TβRIII (sTβRIII), or 3 μm of the ALK5 inhibitor, SB431542, were added at the time of seeding onto the top chambers of the transwell filters. For Nocodazole treatment, cells were pretreated for 1 h with 20 μm before conducting migration assays.

Live Cell Imaging. A Zeiss Axio Observer Z1 motorized microscope equipped with 20, 40, and 100× objective lenses was used for the imaging. Time-lapse recording started either 24 h or 48 h (for infected cells) after plating. The images were collected at 1-min intervals over 120 min with a cooled charge-coupled device (CCD) video camera (Coolsnap ES high resolution CCD camera) operated by Metamorph image analysis software (Molecular Devices). The motility parameters, including migration path, distance, rate, and directional persistence, were obtained from time-lapse movies. Cells were manually traced for each frame using Metamorph to track the migration path of individual cells. The migration paths were expressed as graphs using the Microsoft Excel program. The velocity of cell migration was calculated as a ratio of the total length of migration paths and the duration of migration. The migration distances were determined as the net translocation during a 120-min period. The directional persistence was calculated as a ratio of the direct distance during a 120-min period and the total length of the migration path.

Cdc42 and Rac1 Pull-Down Assays. Briefly, 100,000–200,000 cells were plated in 60-mm dishes, infected with indicated constructs for 48 h, serum-starved for 24 h, then TGF-β1-treated for the indicated times, lysed in 200 mM NaCl, 50 mM Tris (pH 7.5), 10 mM MgCl2, 1% Nonidet P-40, 5% glycerol, and protease inhibitors 50 μg/mL pepstatin, 100 μg/mL leupeptin, and 1 mM PMSF. The cell lysates were cleared after lysis and 5% of lysate used to assess total Cdc42 and Rac1. The remaining lysate was incubated with 25 μg of PAK-CRIB coupled to glutathione-Sepharose 4B beads for 1 h with tumbling at 4 °C. The beads were washed, resuspended in SDS/PAGE sample buffer, and analyzed by Western blot with anti-Cdc42 antibody or anti-Rac1 antibody.

Reverse Transcription and PCR. RNA was isolated from cells using the RNAEasy kit (Qiagen), reverse-transcribed using an oligodT primer (Invitrogen), and then PCR was performed using primers specific for GAPDH, N-cadherin, Slug, Vimentin, and type III TGF-β receptor (TβRIII) as described elsewhere (4). The products were analyzed on a 2% agarose gel, and images were acquired with a Bio-Rad Gel Doc. All assays were performed at least 3 times and results from 1 experiment are provided.

1. Edlund S, Landstrom M, Heldin CH, Aspenstrom P (2002) Transforming growth factor beta-induced mobilization of actin cytoskeleton requires signaling by small GTPases Cdc42 and RhoA. *Mol Biol Cell* 13:902–914.
2. Bayless KJ, Davis GE (2002) The Cdc42 and Rac1 GTPases are required for capillary lumen formation in three-dimensional extracellular matrices. *J Cell Sci* 115:1123–1136.
3. Girnita L, et al. (2007) Beta-arrestin and Mdm2 mediate IGF-1 receptor-stimulated ERK activation and cell cycle progression. *J Biol Chem* 282:11329–11338.
4. Gordon KJ, Dong M, Chislock EM, Fields TA, Blobe GC (2008) Loss of type III transforming growth factor beta receptor expression increases motility and invasiveness associated with epithelial to mesenchymal transition during pancreatic cancer progression. *Carcinogenesis* 29:252–262.

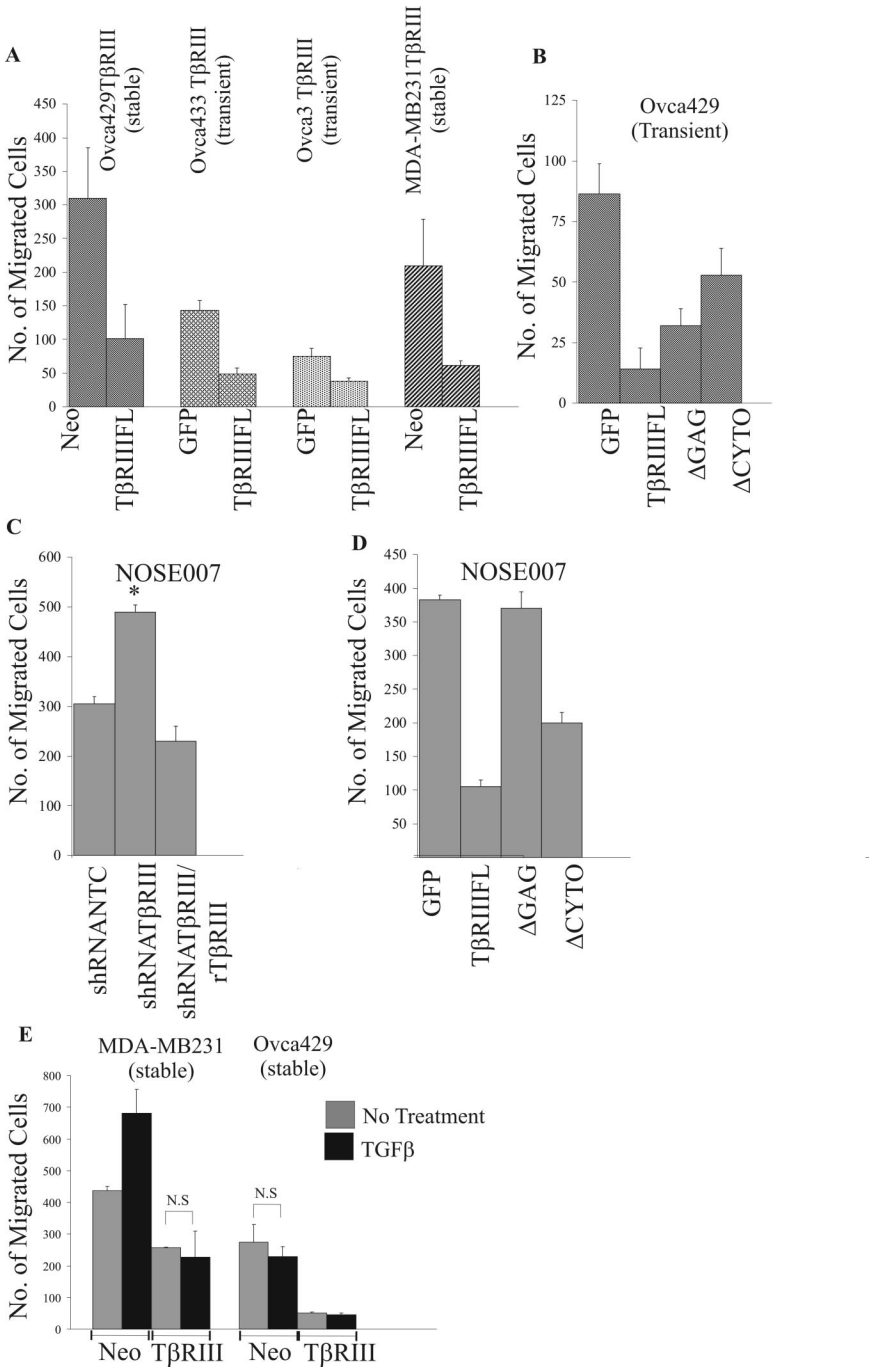

Fig. S1. TβRIII inhibits cell migration in epithelial and cancer cells. (*A*) Cancer cell lines stably expressing full-length TβRIII (TβRIIIFL) with Neo as controls (Ovca429 and MDA-MB231) were seeded at a cell density of 25,000 on fibronectin-coated filters, and cancer cell lines transiently expressing TβRIIIFL with GFP as control (Ovca433 and Ovca3) were seeded at a cell density of 25,000 and 30,000, respectively, on fibronectin-coated filters and allowed to migrate for 18–24 h toward 10% FBS in the lower chamber. Cells migrating through the fibronectin layer were visualized as described in *Materials and Methods*, and 3 images per filter were quantified with each column representing the mean ± SE. Data are a composite of 3 experiments. (*B*) Transwell migration of Ovca429 cells transiently expressing either TβRIIIFL, TβRIIIΔGAG (lacking the glucosaminoglycan chains), or TβRIIIΔCYTO (lacking the cytoplasmic domain) relative to GFP control was conducted by plating 20,000 cells in serum-free media (SFM) in the top chamber of a transwell and allowing them to migrate for 18–24 h toward 10% FBS. Data represent the mean ± SE of 3 independent experiments performed in triplicate. (*C*) We plated 45,000 normal ovarian surface epithelial (NOSE007) cells in SFM in the top chamber of a transwell and allowed them to migrate for 18–24 h toward 10% FBS 72 h after infection with adenovirus-expressing shRNA non-targeting control (NTC), human shRNA-TβRIII alone, or human shRNA-TβRIII after infection with rat TβRIIIFL (rTβRIIIFL). The number of migrated cells is presented and data are a composite of 3 experiments. *, $P = 0.0036$, relative to control. (*D*) We plated 45,000 NOSE07 cells in SFM in the top chamber of a transwell and allowed them to migrate for 18–24 h toward 10% FBS 48 h after infection with adenovirus-expressing GFP as control, TβRIII, TβRIIIΔGAG, or TβRIIIΔCYTO. Data represent the mean ± SE of 3 independent experiments performed in duplicate. (*E*) MDA-MB231Neo, MDA-MB231TβRIII, Ovca429Neo, and Ovca429TβRIII stable cell lines were treated with 200 pM TGF-β1 in the top chamber at the time of seeding and transwell migration was conducted as described.

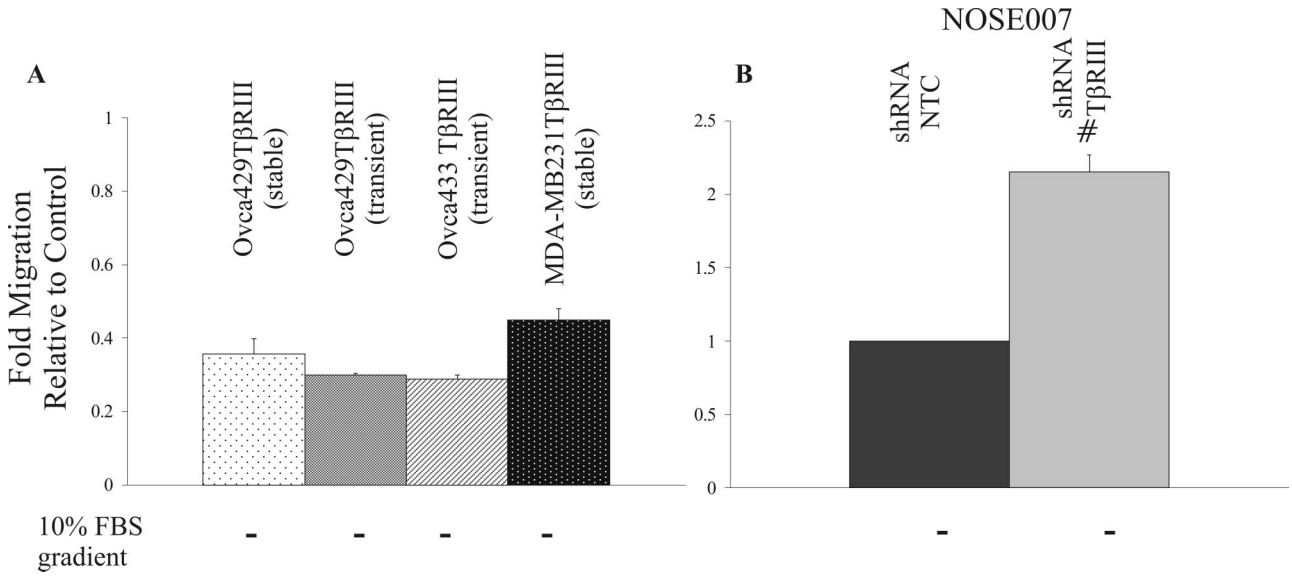

Fig. S2. TβRIII suppresses the intrinsic migration of epithelial and cancer cells. (*A*) Cancer cell lines either stably-expressing TβRIIIFL (stable) or the indicated cancer cell lines transiently expressing TβRIIIFL by adenoviral infection with GFP vector controls (transient) were subjected to transwell migration in the absence of a 10% FBS gradient. Cells were plated in SFM in the top chamber and allowed to migrate for 18–24 h. Fold migration in all TβRIII cells relative to control (Neo-expressing control for stable lines and adenoviral-infected GFP-vector control cells for transient expression) is presented. Data are a composite of 3 independent experiments with each performed in triplicate. Each column represents the mean ± SE. (*B*) Transwell migration in the absence (−) of a 10% FBS gradient was assessed 72 h after infecting NOSE007 cells with adenovirus-expressing shRNA-TβRIII, or shRNA NTC and dsRed. Fold migration relative to shRNA NTC is presented. #, $P < 0.0001$.

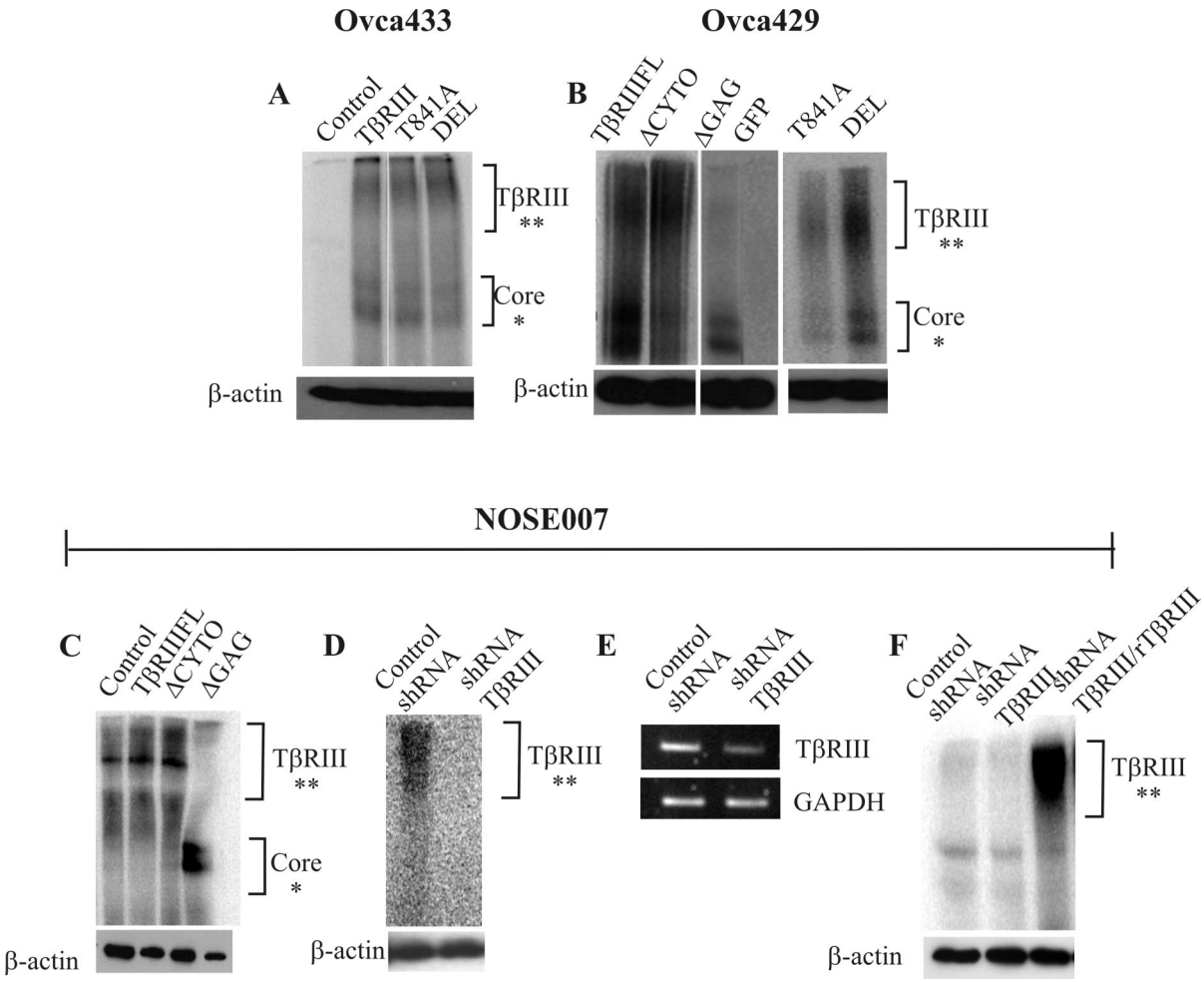

Fig. S3. Verification of TβRIII expression, TβRIII knockdown, and rescue. (*A–C*) Verification of expression of TβRIII constructs. Expression of the indicated TβRIII constructs in Ovca433 (*A*), Ovca429 (*B*), and NOSE007 cells (*C*). Forty-eight hours after infecting with adenovirus-expressing GFP-tagged construct TβRIIIFL, TβRIIIΔCYTO, TβRIIIΔGAG, TβRIII-T841A (TβRIII mutant unable to bind β-arrestin2), TβRIII-DEL (TβRIII mutant unable to bind GIPC), or GFP alone as control, expression was detected by ^{125}I-TGF-β1 binding and crosslinking. Lanes in *B* are from the same experiment and same exposure but have been rearranged for clarity. *, position of the TβRIII protein core; **, TβRIII protein containing glycosaminoglycan modifications. (*D–E*) Verification of shRNA-mediated silencing of TβRIII expression. The effect of shRNA-TβRIII relative to shRNA NTC (control shRNA) on cell surface TβRIII expression in NOSE007 cells; 72 h after infecting with adenovirus-expressing, these constructs and dsRed followed by lysis and immunoprecipitation with antibody to TβRIII followed by detection by ^{125}I-TGF-β1 binding and crosslinking. (*E*) Reverse transcription and RT-PCR for TβRIII was carried out as stated in *Materials and Methods* to verify knockdown of TβRIII expression at the mRNA level. GAPDH was used as a control. (*F*) Rescue of cell-surface expression of rat TβRIII (rTβRIII) after shRNA-mediated silencing of TβRIII expression. Forty-eight hours after infection with shRNA-TβRIII, cells were infected with rTβRIII for an additional 48 h and cell-surface expression was verified by ^{125}I-TGF-β1 binding and crosslinking. In all cases β-actin was used as a loading control.

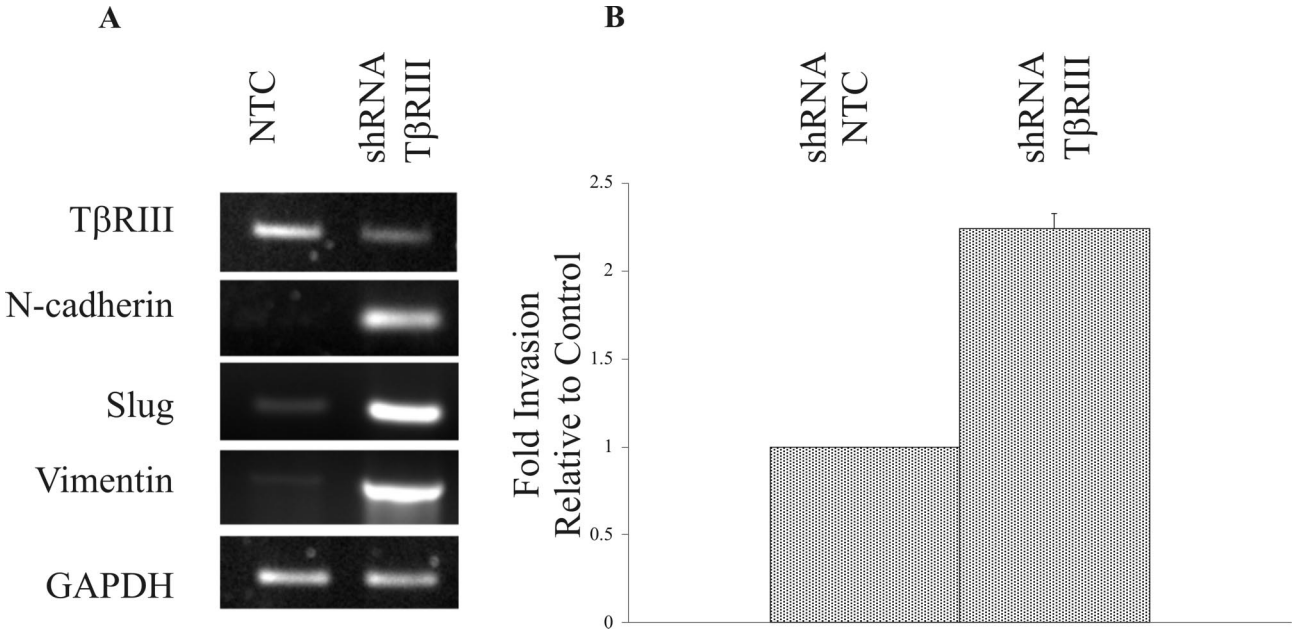

Fig. S4. Reduction of TβRIII NOSE007 cells is associated with increased expression of epithelial to mesenchymal transition markers and invasive potential. NOSE007 cells were infected with an adenovirus-expressing shRNA to TβRIII or a NTC shRNA as described in *Materials and Methods*. (*A*) After 72 h of infection, RNA was isolated from the cells, reverse transcribed, and PCR was performed with primers specific for TβRIII, N-cadherin, Slug, and GAPDH. (*B*) Invasion assays were performed by using Matrigel-coated transwells as described in *Materials and Methods*.

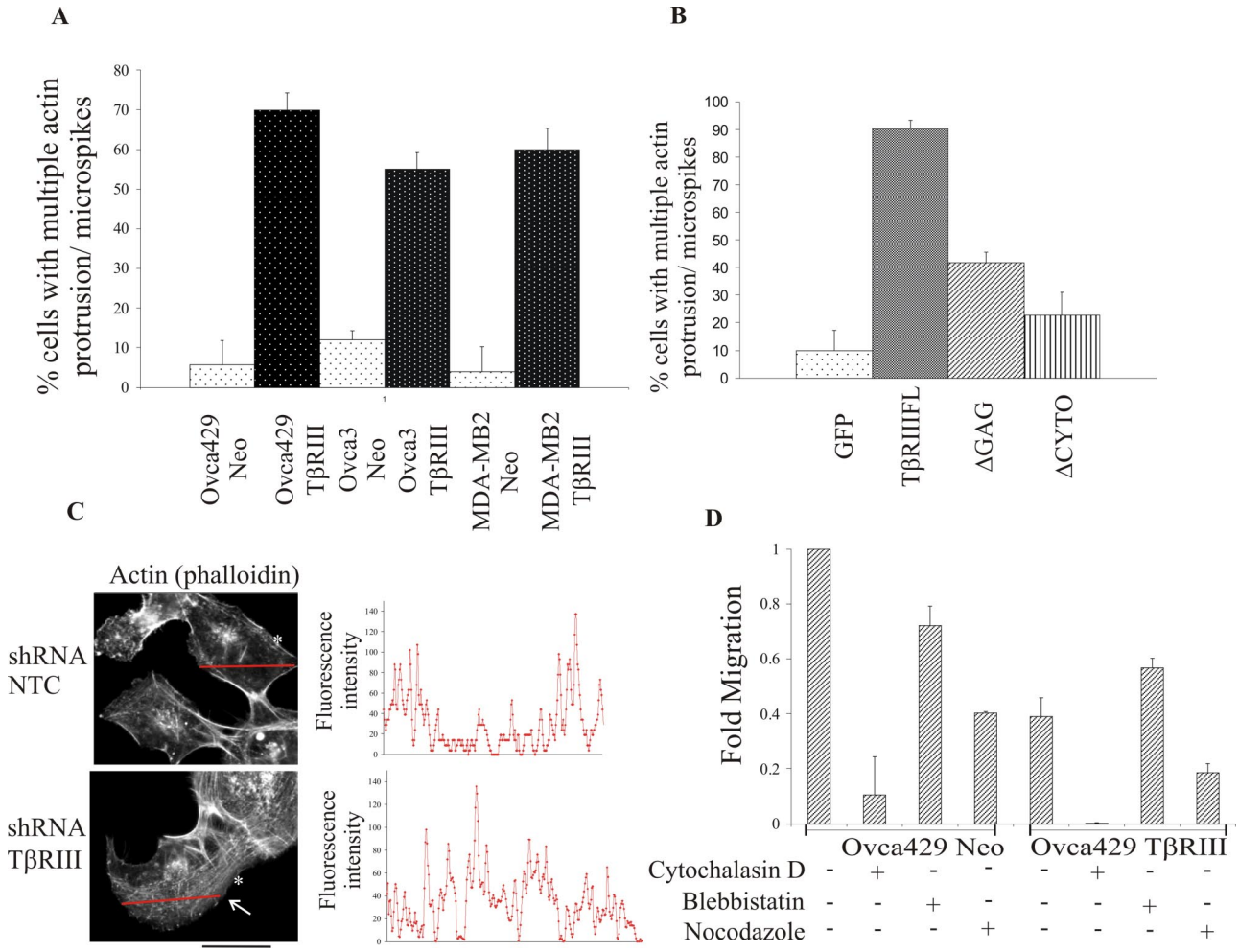

Fig. S5. TβRIII alters the actin cytoskeletal organization of epithelial and cancer cells. (*A*) We plated 5–8 × 10^4 of the indicated cancer cell lines on coverslips and stained for actin by using rhodamine phalloidin. For cells transiently expressing TβRIII, subconfluent cells were infected with adenovirus-expressing control (GFP) or TβRIII and GFP; the cells were fixed and stained 48 h after infection, and only GFP-expressing cells were examined. Quantitation of percentage of cells exhibiting multiple actin protrusions/microspikes per cell was calculated and plotted. Cells with protrusions longer than 5 μm and ≥8 protrusions per cell for Ovca429 and Ovca3 and ≥4 protrusions per cell for MDA-MB231 cells were considered to have the multiple actin protrusion/microspike phenotype. Data presented are mean ± SE, $n \geq 150$ per cell line. (*B*) After 48 h of infecting Ovca429 cells with adenovirus-expressing GFP, TβRIIIFL, TβRIIIΔGAG, or TβRIIIΔCYTO cells were fixed and stained for actin using rhodamine phalloidin. GFP-expressing cells were examined and quantitation of the percentage of cells exhibiting microspike structures across the entire cell surface under different conditions was calculated and plotted. Data presented are mean ± SE, $n \geq 150$ per condition. (*C*) Quantification of fluorescence intensity using ImageJ software across the lines shown in the corresponding panels on the left are indicative of stress-fiber density. Asterisks demarcate cells being quantified and their corresponding line graphs on the right. (*D*) Ovca429Neo and Ovca429TβRIII cells were treated with the indicated pharmacological agents as indicated (see *Materials and Methods*) and transwell migration toward 10% FBS was assessed. Data are a composite of 2 independent experiments performed in triplicate. Each column represents the mean ± SE.

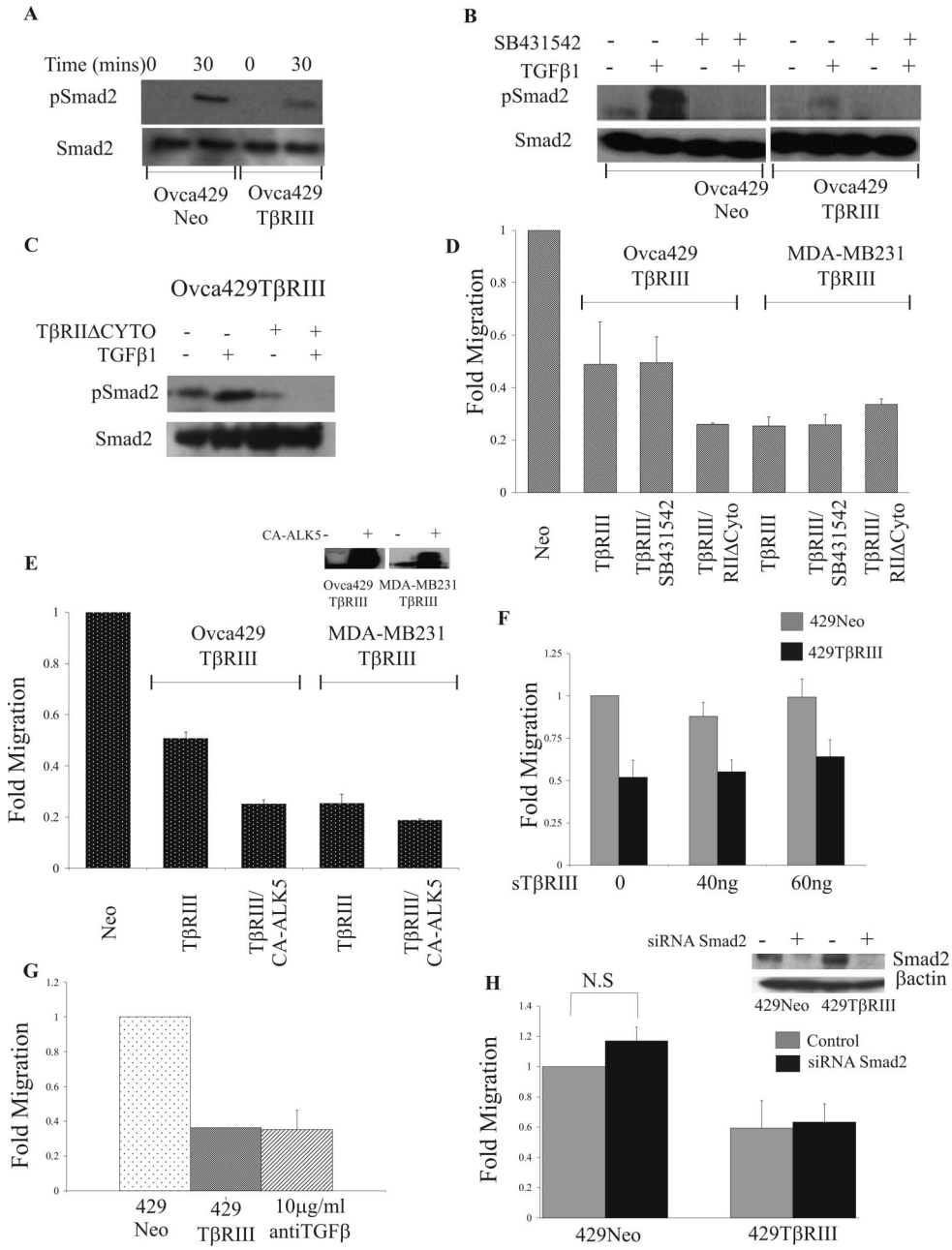

Fig. S6. TβRIII-mediated suppression of migration is independent of the TβRII/TβRI/Smad2 signaling pathway. (*A*) Ovca429Neo and Ovca429TβRIII cells were treated with TGF-β1 (200 pM) for the indicated times and the resulting cell lysates were analyzed with pSmad2 and total Smad2 antibodies. (*B*) Ovca429Neo and Ovca429TβRIII cells were treated with TGF-β1 (200 pM) with and without SB431542 (3 μm) and the resulting cell lysates were analyzed with a pSmad2 and total Smad2 antibodies. (*C*) Validation of the ability of TβRIIΔCYTO to block TGF-β1/Smad signaling. After 48 h of transiently transfecting Ovca429TβRIII cells with TβRIIΔCYTO, cells were stimulated with TGF-β1 (200 pM) for 30 min, and cell lysates were assessed for pSmad2. Total Smad2 was used as a loading control. (*D*) Transwell migration of the indicated cell lines toward a 10% FBS gradient was assessed either in the presence of SB431542 (3 μm) or DMSO control in the top chamber or 48 h after transfecting Ovca429TβRIII and MDA-MB231TβRIII cells with TβRIIΔCYTO expression vector. Fold migration is presented. (*E*) Transwell migration of indicated cell lines toward a 10% FBS gradient was assessed 48 h after transfecting Ovca429TβRIII and MDA-MB231TβRIII cells with CA-ALK5 expression vector. Fold migration is presented. (*C* and *D*) Data are a composite of 2 independent experiments with each performed in triplicate. Each column represents the mean ± SE. (*F*) sTβRIII does not alter TβRIII-mediated inhibition of migration. Transwell migration of indicated cell lines toward a 10% FBS gradient was assessed in the presence of 40 ng or 60 ng sTβRIII in the top chamber. Fold migration is presented. (*G*) Pan-neutralizing-TGF-β antibody does not alter TβRIII-mediated inhibition of migration. Transwell migration of indicated cell lines toward a 10% FBS gradient was assessed either in the presence or absence of pan-neutralizing-TGF-β antibody in the top chamber. Fold migration is presented. (*H*) siRNA to Smad2 was conducted in Ovca429Neo and Ovca429TβRIII cells as described in *Materials and Methods* for 48 h followed by transwell migration as described in *D–F*. Fold migration relative to Neo-control cells is presented. Data are a composite of 2 experiments with each performed in duplicate. Each column represents the mean ± SE.

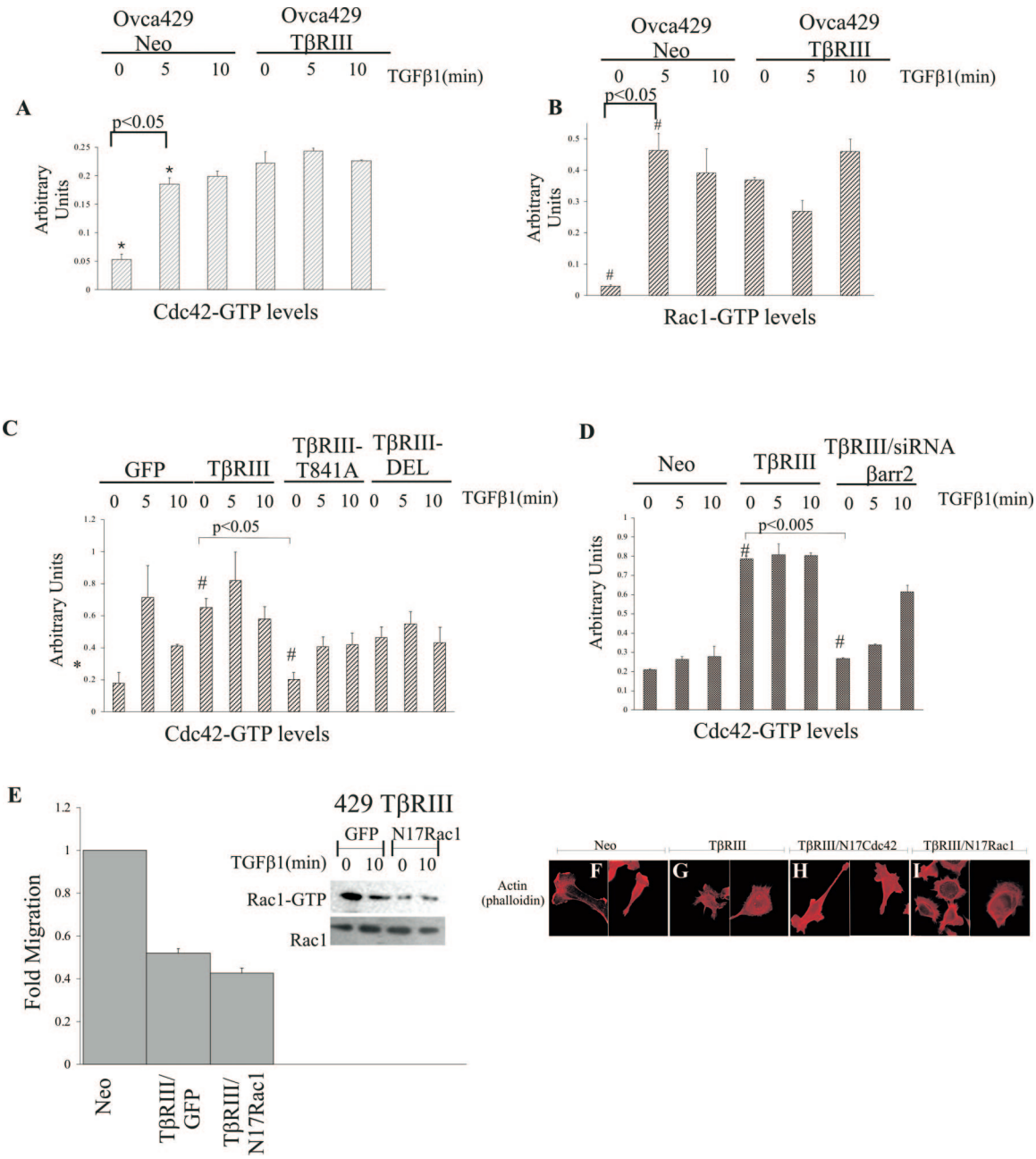

Fig. S7. TβRIII inhibits motility through constitutive activation of Cdc42. Ovca429Neo and Ovca429TβRIII cell lines were serum-starved for 16 h followed by stimulation with TGF-β1 (200 pM) for the times indicated and pull-down assays for active Cdc42 and Rac1 were performed. Five percent of lysate was assessed for effects on total Cdc42 and Rac1 levels. Quantification of amount of active Cdc42 (*A*) or Rac1 (*B*) was determined by using ImageJ software and represented as fold-change-normalized to total Cdc42 and Rac1. The graph is the average of 2 independent experiments, and columns represent mean ± SE (*, $P = 0.0114$ and #, $P = 0.0156$). (*C*) Forty-eight hours after infecting Ovca429 cells with adenovirus-expressing GFP, TβRIIIFL, TβRIII-T841A, or TβRIII-DEL cells were serum-starved for 16 h followed by stimulation with TGF-β1 (200 pM) for the times indicated and pull-down assays for active Cdc42 were conducted. Five percent of lysate was assessed for effects on total Cdc42 levels. Quantification of amount of active Cdc42 was determined by using ImageJ software and is represented as fold-change-normalized to total Cdc42. The graph is the average of 2 independent experiments and columns represent mean ± SE (#, $P = 0.0348$). (*D*) Seventy-two hours after infecting Ovca429 TβRIII cells with either control DNA or siRNAβ-arrestin2, cells were serum-starved and Cdc42-GTP levels determined as described above. Quantitation was performed as described above and is represented as fold-change-normalized to total Cdc42. The graph is the average of 2 independent experiments and columns represent mean ± SE (#, $P = 0.0034$). (*E*) Efficacy of N17Rac1 was determined by infecting cells as described in *Materials and Methods*. Forty-eight hours after infection, cells were either used for transwell migration assays or serum-starved for 16 h followed by stimulation with TGF-β1 (200 pM) for the times indicated and pull-down assays for active Rac1 and transwell migration assays were conducted as described (*Materials and Methods*). (*F–I*) Ovca429Neo and Ovca429TβRIII cells infected with adenovirus expressing either GFP-N17Cdc42 (*H*) or GFP-N17Rac1 (*I*) were fixed and stained for actin by using rhodamine phalloidin. GFP-expressing cells were examined and representative examples are presented.

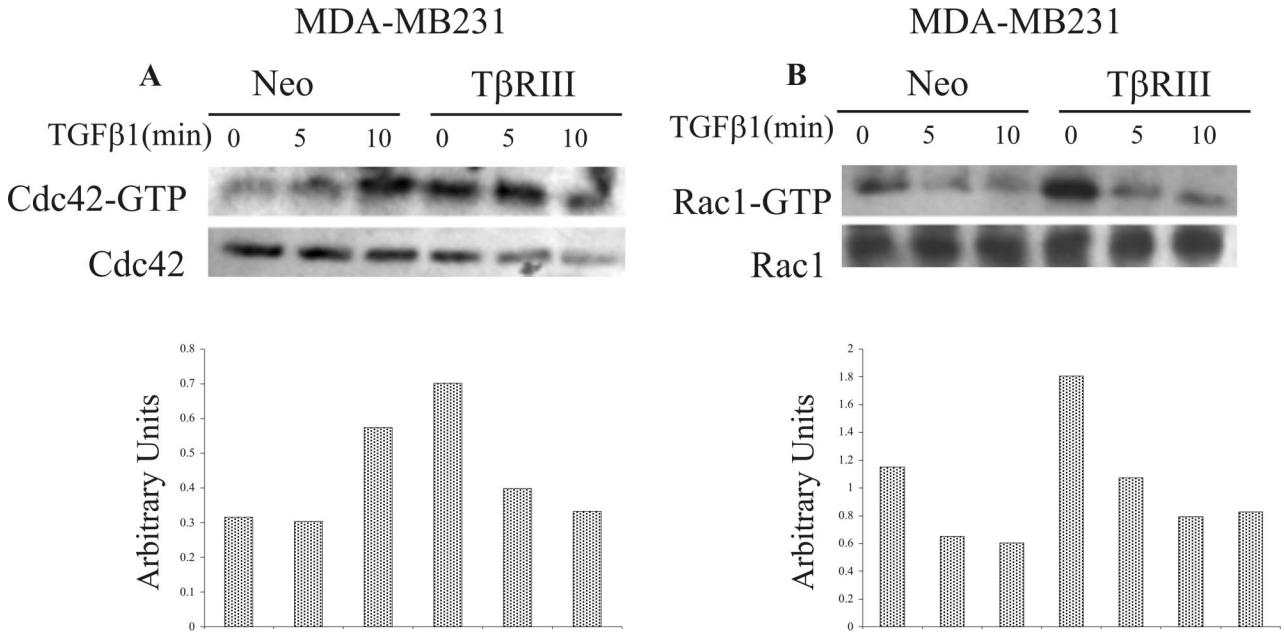

Fig. S8. TβRIII inhibits motility through constitutive activation of Cdc42 in the MB-MDA231 breast cancer cell line. MDA-MB231Neo and MDA-MB231TβRIII cell lines were serum-starved for 16 h followed by stimulation with TGF-β1 (200 pM) for the times indicated and pull-down assays for active Cdc42 (*A*) and Rac1 (*B*) were performed. Five percent of lysate was assessed for effects on total Cdc42 and Rac1 levels. A representative experiment of 2 independent experiments is presented. Quantification of amount of active Cdc42 was determined by using ImageJ software and is represented as fold-change-normalized to total Cdc42 or Rac1.

Movie S1. Ovca429Neo.

Movie S1 (AVI)

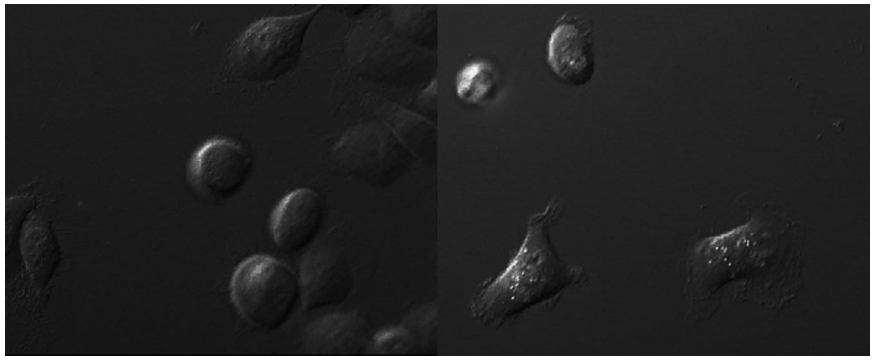

Movie S2. Ovca429TβRIII.

Movie S2 (AVI)

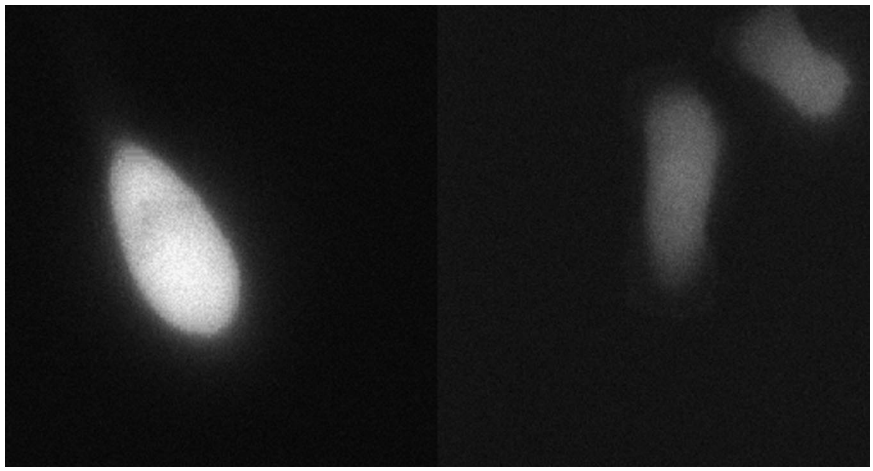

Movie S3. Ovca429TβRIII/N17Cdc42.

Movie S3 (AVI)